2017

A Route to Surface-bound Metalloporphyrins as Models for Oxygen Reduction Catalysts

Stephen J. Van Wyck
University of Vermont

A Route to Surface-bound Metalloporphyrins as Models for Oxygen Reduction Catalysts

Stephen J. Van Wyck
Advisor William E. Geiger

Abstract:

The attachment nonmetal and magnesium ethynyl terminated porphyrin (TEPP and MgTEPP) to glassy carbon electrode was achieved through voltammetry. These attached porphyrins were studied by cyclic voltammetry (CV) and UV-visible spectroscopy. Surface-bound TEPP displayed reversible oxidation and reduction ($E_{1/2}$ = 0.52 V and $E_{1/2}$ = -1.74 V vs. ferrocene), and absorbance peak of 425 nm on indium tin oxide (ITO). While surface-bound MgTEPP possessed two reversible oxidations ($E_{1/2}$ = 0.61 V and $E_{1/2}$ = 0.97 V vs. Ag/AgCl) and an irreversible (E_{pc} = -1.65 V vs. Ag/AgCl). MgTEPP had an absorbance maximum at 431 nm on ITO. Both porphyrins had irreversible pre-waves, which could be regenerated. This is the first example of covalently-bound Mg porphyrin to an electrode surface.

Acknowledgements: I would like to thank my advisor, Prof. William E. Geiger, for his unceasing support and guidance through my three and half years in his group. I would also like to thank my committee members, Prof. Peter Dodds and Prof. Rory Waterman. This research was funded by the National Science Foundation (under grants NSF-CHE 1212339 and CHE 1565541).

Table of Contents:

Table of Tables:

Table of Figures:

Introduction:

The proliferation of hydrogen cells has been hindered for years by their requirement for platinum catalysts, due its high cost and low availability.[1] Despite the expense, this technology has been used in specialized applications such as powering the electrical systems of Apollo spacecraft.[2]

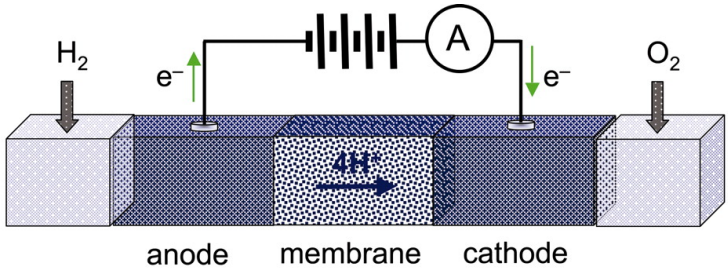

Scheme 1: Simplified diagram of a hydrogen fuel cell (Ref. 3).

Inside a hydrogen fuel cell, molecular oxygen is reduced and molecular hydrogen is oxidized to produce only water and electricity. The reactions are shown with the following equations.

Anode Reaction: $2H_2 \rightarrow 4H^+ + 4e^-$

Cathode Reaction: $O_2 + 4H^+ + 4e^- \rightarrow 2H_2O$

Overall Reaction: $O_2 + 2H_2 \rightarrow 2H_2O$

The cathode reaction, or oxygen reduction reaction (ORR), is sluggish, due to the large kinetic barrier, unless a platinum electrode is used. There is a need for cheaper and more abundant metals as catalysts to increase the availability of fuel cells. Over the years, cobalt-based porphyrin catalysts have emerged as promising alternatives to platinum catalysts, showing limited production hazard and damaging hydrogen peroxide.[3] Despite the low production of hydrogen peroxide, further work is required to reduce the overpotentials.

Presented here is research towards the goal of producing cobalt porphyrins covalently bonded to an electrode. Protonated and metallated porphyrins were studied. Tetra-phenylporphyrins (TPPs) were synthesized and characterized by electrochemistry to facilitate the understanding of ethynyl terminated porphyrins, tetra(ethynyl-phenyl)-porphyrin. It has been previously demonstrated that porphyrins with terminal ethynyl groups can be covalently attached to a glassy carbon electrode through oxidation of their ethynyl groups.[4] A single-electron oxidation of the ethynyl group leads to loss of a proton and the formation of a neutral carbon radical. This radical reacts with the glassy carbon surface to form a new covalent carbon-carbon bond, between the molecule and the electrode. This technique offers a simple and robust method of attachment, allowing the formation of ordered layer(s) of porphyrin species. The synthesis of surface-bound cobalt porphyrins was explored in this research. A synthetic route that was investigated was the

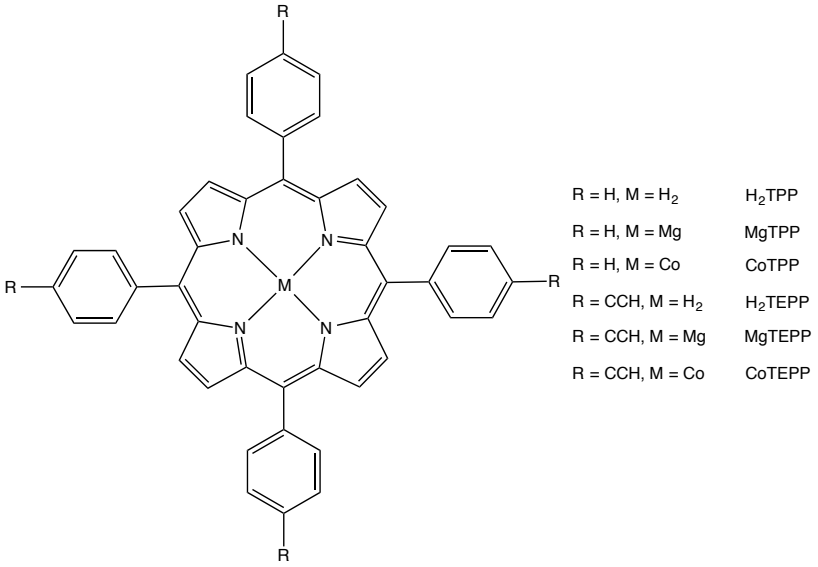

Scheme 2: Porphyrins involved in this study.

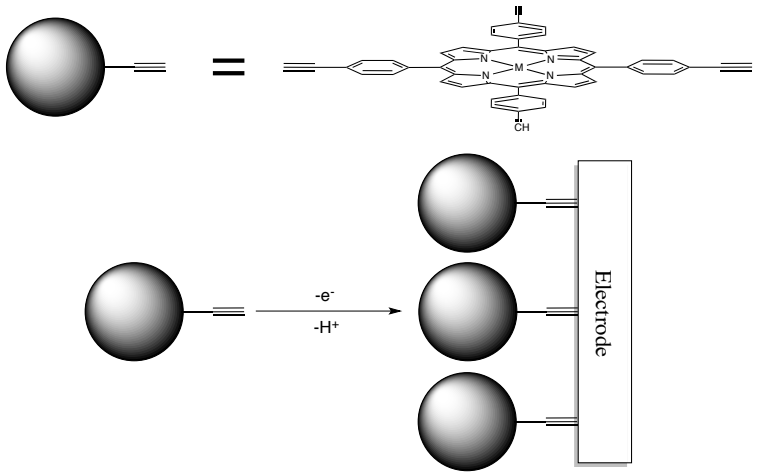

Scheme 3: Attachment of porphyrins to the electrode

exchange of larger metal ions to produce cobalt porphyrins. Metal exchange have been shown to be 600 – 6700 times faster than preparation from protonated porphyrin.[5] Magnesium porphyrins was used in this study because of its ease of preparation and magnesium's covalent radius.[6] The exchange of magnesium was found to be too sluggish under the condition used. Future research will vary the reaction condition and investigate the exchange of cadmium.

Experimental:

Materials:

The materials were used as received unless otherwise noted. Commercial sources were used for: pyrrole (Sigma-Aldrich, St. Louis, MO, dried over CaH_2 and distilled), 4-((trimethylsilyl) ethynyl)-benzaldehyde (Alfa Aesar, Ward Hill, MA), boron trifluoride diethyl etherate (Acros, Ceel, Belgium), *p*-chloranil (Alfa Aesar, Heysham, United Kingdom), potassium carbonate (Aldrich, Milwaukee, WI), tetraphenylporphyrin (H_2TPP) (1-3% chlorin impurity, Frontier Scientific, Newark, DE), magnesium bromide diethyl etherate (Acros, Ceel, Belgium), triethylamine (Acros, Ceel, Belgium), anhydrous cobalt(II) chloride (Aldrich, Milwaukee, WI), silica gel (Sorbtech, Norcross, GA) and $[NBu_4][PF_6]$ (Tokyo Chemical Industry). Dichloromethane for electrochemistry was purified and dried by passing it through an alumina-based solvent system under argon.

Instrumentation:

Electrochemistry:

The electrochemistry was carried out under nitrogen atmosphere in a Vacuum Atmospheres drybox. Three-electrode cells were used for voltammetry experiments. A platinum wire was used as the counter-electrode and was separated from the working compartment with a fine-porosity

frit. For use as the experimental reference electrode, a silver wire electroplated with silver chloride was used. This electrode was separated from the working compartment by another fine-porosity frit. Each working electrode, a glassy carbon (GC) disk 2 mm in diameter, was purchased from Bioanalytical Systems. Before each experiment, the electrodes were polished with diamond paste and washed with nanopure water and acetone. Potentials are reported versus the ferrocene/ferrocenium couple[7] and were found by the *in situ* method.[8] The potentiostat employed was EG&G PARC 273. All experiments were performed at ambient temperature.

UV-visible spectroscopy:

Solution-phase spectra were obtained in dichloromethane using a cell with a 1 cm path length. For surface spectra, the porphyrins were deposited on an indium tin oxide (ITO) slide. A background spectrum of the ITO slide was collected and then subtracted from the spectrum of the modified slide. An Olis 14 UV/VIS/NIR spectrophotometer was used for the UV-vis measurements.

Procedures:

Synthesis of tetra(trimethylsilyl-ethynyl-phenyl)-porphyrin (TTMSEPP)[9]:

Pyrrole (0.14 mL, 2.0 mmol) and 4-((trimethylsilyl)ethynyl)benzaldehyde (0.420 g, 2.1 mmol) were added to a 1000-mL round bottom flask (rbf). Dichloromethane (350 mL) and boron trifluoride diethyl etherate (70 μL, 0.55 mmol) were added to the rbf, yielding an orange solution. The solution was stirred under nitrogen at room temperature for three hours, yielding a reddish solution. Next, *p*-chloranil (0.377 g, 1.53 mmol) was added to the rbf. The solution was refluxed for one hour, yielding a nearly black solution. The solvent was evaporated, and the solids were re-dissolved in the minimum amount of acetone. Silica gel (5 mL) was added to the acetone solution,

and the acetone was evaporated, leaving the solids on the silica gel. A 2-cm diameter column was filled with silica gel, and the silica gel with product was added on top. The product was purified on silica gel with dichloromethane as the eluent. The elution was followed by thin layer chromatography. The dichloromethane was evaporated yielding 240 mg (48.0%) porphyrin. UV-vis (dichloromethane): λ_{max} = 422 nm.

Synthesis of tetra(ethynyl-phenyl)-porphyrin (TEPP)[9]:

TTMSEPP (0.240 g, 0.240 mmol) was dissolved in a dichloromethane-methanol mixture (3:1, 20 mL). Potassium carbonate (0.192 g, 1.39 mmol) was added to the solution. The mixture was stirred under nitrogen at room temperature overnight. The solvents were removed *in vacuo*, and the solid was re-dissolved in dichloromethane (40 mL). The solution was washed with 10% aqueous sodium bicarbonate (60 mL) and dried with magnesium sulfate. The solvent was evaporated, and the solids were re-dissolved in acetone. Silica gel (5 mL) was added to the acetone solution, and the acetone was evaporated, leaving the solids on the silica gel. A 2-cm diameter column was filled with silica gel, and the silica gel with product was added on top. Product was eluted with 7:3 (v/v) dichloromethane-hexanes. The elution was followed by thin layer chromatography. The solvents were evaporated yielding 41 mg (24.1%) porphyrin. UV-vis (dichloromethane): λ_{max} = 421 nm. ^{1}H NMR (500 MHz, $CDCl_3$, δ in ppm): 8.82 (s, 8H, $H_{\beta\text{-pyrrolic}}$), 8.15 (d, 8H, H_{Ar}), 7.87 (d, 8H, H_{Ar}), 4.24 (s, 4H, C_2H), –2.88 (s, 2H, N*H*).

Homogenous synthesis of magnesium tetra-phenylporphyrin (MgTPP)[10]:

TPP (0.117 g, 0.190 mmol) was dissolved in dichloromethane (10 mL). Magnesium bromide ethyl etherate (0.736 g, 2.85 mmol) was ground and added to the solution with triethylamine (0.5 mL, 3.58 mmol). The suspension was stirred at room temperature under nitrogen

for 4.5 hours. The suspension was diluted with dichloromethane (25 mL) and then washed with 5% aqueous sodium carbonate (2 × 25 mL). The dichloromethane solution was separated and dried with magnesium sulfate. The dichloromethane was evaporated, and the solids were re-dissolved in the minimum amount of dichloromethane. A 2-cm diameter column was loaded with silica gel, and the product solution was added. The residue was purified on silica with 9:1 (v/v) hexanes-ethyl acetate as the eluent. The elution was followed by thin layer chromatography. The solvents were evaporated yielding 113 mg (93.2%) porphyrin. UV-vis (dichloromethane λ_{max} = 426 nm).

Homogenous synthesis of cobalt tetra-phenylporphyrin (CoTPP)[11]:

TPP (48 mg, 0.078 mmol) was dissolved in methanol (10 mL). Anhydrous cobalt chloride (104 mg, .801 mmol) was dissolved in chloroform (15 mL). The solutions were combined, and the solution was refluxed for 3.5 hours. The solution was washed with a saturated aqueous sodium chloride solution (2 × 25 mL) and was dried with sodium sulfate. The organic solvent was evaporated. The yield was 53 mg (100%). UV-vis (dichloromethane λ_{max} = 411 nm).

Electrode modification:

Using glassy carbon electrodes, cyclic voltammetry was performed on solutions containing an analyte with a terminal ethynyl group. Electrode modification was achieved by applying potentials greater than the oxidation potential of the ethynyl group. To maximize surface coverage, successive scans were used. The modified electrodes were washed with acetone and sonicated in dichloromethane for two minutes. The electrodes were electrochemically analyzed by performing voltammetry in a solution containing only supporting electrolyte. When ITO slides were used, they were tested by UV-vis, by obtaining scans before and after modification with the porphyrin.

Hetrogenous synthesis of magnesium tetra(ethynyl-phenyl)-porphyrin (MgTEPP):

Magnesium bromide ethyl etherate (0.796 g, 2.85 mmol) was suspended in dichloromethane (10 mL). Triethylamine (0.5 mL, 3.58 mmol) was added to the suspension. An electrode modified with TEPP was fixed overnight in the suspension while it stirred. The electrode was added with acetone and sonicated in dichloromethane for two minutes, yielding a clean electrode modified with MgTEPP (30% yield, compared to original surface coverage).

Results:

Experiments were first performed with synthetic preparation and electrochemistry of magnesium and cobalt metalloporphyrins. The tetraphenylporphyrin (H_2TPP) was purchased commercially. MgTPP and CoTPP were prepared by published methods,[10-11] already outlined in this report. These non-ethynyl terminated porphyrins were used to aid the preparation and characterization of the ethynyl terminated porphyrins, which have been studied far less in the literature (Scheme 4).

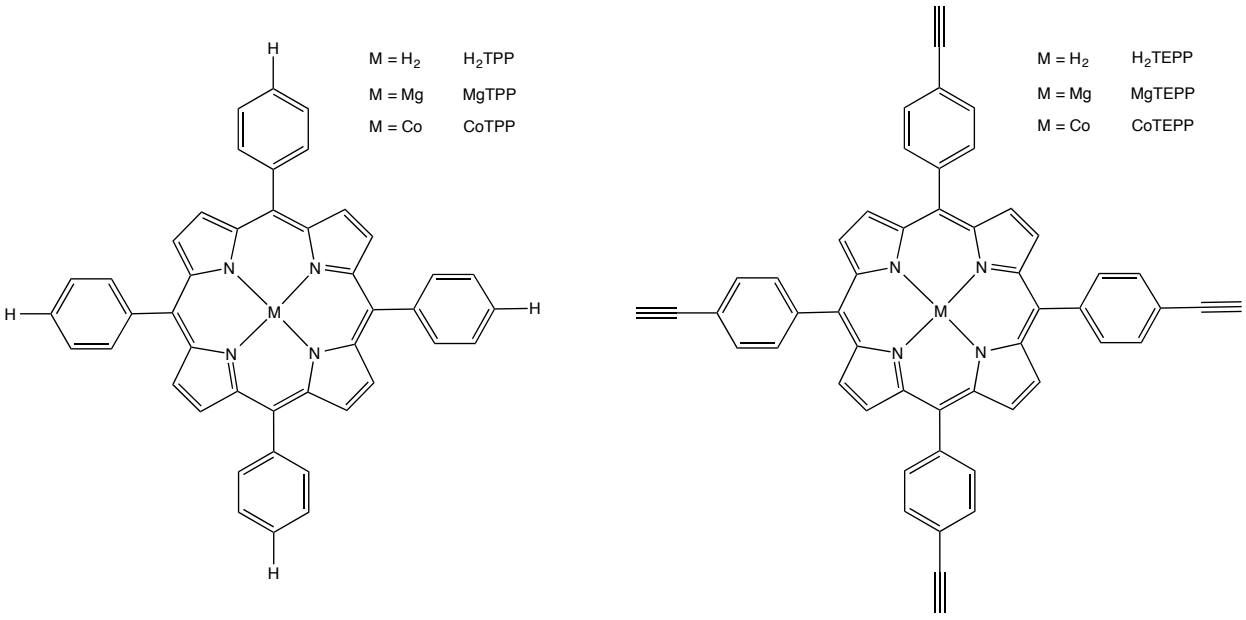

Scheme 4: Non-ethynyl terminated porphyrin (left) and ethynyl terminated porphyrin (right).

Synthesis of CoTPP was also attempted from MgTPP. Thus, MgTPP (1.9 mM) and anhydrous cobalt chloride (0.10 M) were stirred in 1:1 dichloromethane-methanol solution at room temperature. Figure 1 shows the UV-vis spectrum of MgTPP initially (blue) and 24 hours after addition of cobalt chloride (red). In both cases, the Soret band appears at 426 nm, which is consistent with MgTPP.[12] The Soret band for CoTPP appears at 411 nm. Therefore, these data show that replacement of the Mg by Co had not occurred.

Figure 2 displays the cyclic voltammetry of H_2TPP. H_2TPP yielded three reversible oxidations, the third of which is less prominent (Fig. 2, solid line). The first oxidation wave ($E_{1/2}$ = 0.54 V) shows the characteristics of a one-electron reversible system ($E_{pa} - E_{pc}$ = 80 mV, $E_p - E_{p/2}$ = 80 mV). The second oxidation wave ($E_{1/2}$ = 0.87 V) has a similar shape and was assumed to also rise from a reversible, one-electron process. These first two one-electron oxidations fall at potentials that are consistent with literature results, indicating successive oxidations of H_2TPP.[13] The third oxidation ($E_{1/2}$ = 1.09 V) has considerably smaller currents compared to the first two oxidations and is likely to rise from the known 1-3% chlorin contaminant in the H_2TPP sample. The two reduction couples ($E_{1/2}$ = –1.70 V, $E_{1/2}$ = –2.02 V) are comparable to the oxidation couples and therefore are assumed to be reversible, one-electron processes (Fig. 2, dashed line).[13] The potentials measured for the redox processes of H_2TPP and its metal derivatives are collected in Table 1.

The oxidation behavior of MgTPP resembled that of H_2TPP (Fig 3). MgTPP displayed two reversible one-electron oxidations ($E_{1/2}$ = 0.19 V, $E_{1/2}$ = 0.56 V).[13c, 14] One chemically irreversible reduction wave (E_{pc} = –1.98 at 0. 2 V/s) has the properties of a one-electron transfer ($E_p - E_{p/2}$ = 80 mV).[13c, 14-15]

CoTPP had more redox waves than the Mg complex (Fig. 4). Three reversible oxidations (Fig. 5, solid line) are present ($E_{1/2}$ = 0.46 V, $E_{1/2}$ = 0.69 V, $E_{1/2}$ = 0.84 V). [14] As with H_2TPP and MgTPP, each of these oxidations is a single-electron process. A partially reversible reduction was observed ($E_{1/2}$ = –1.36 V) (Fig. 4, dashed line). Scans at 200 mV/s and 400 mV/s reveal a dependency of reversibility on the scan rate (i_a/i_c = 0.64 at 200 mV/s and i_a/i_c = 0.75 at 400 mV/s, where i_a/i_c = 1 is fully reversible). The final reduction is irreversible (E_{pc} = –1.90 V) (Fig. 4, dotted line), attributed to the reduction to Co(II). An irreversible oxidation (E_{pa} = –0.74 V) is seen on the back scan, after scanning through the second reduction and perhaps through the first reduction. The smaller redox waves are assumed to be spurious.[14]

After studying the non-ethynyl terminated porphyrins, experiments were performed with the ethynyl terminated porphyrins. Electrochemistry was performed on TEPP with the goal of achieving electrode modification. In homogeneous solution, scanning to 1.2 V (Fig. 5, dashed line), revealed two partially reversible oxidations ($E_{1/2}$ = 0.58 V, $E_{1/2}$ = 0.94 V). The second oxidation has the characteristics of a multi-electron process, along with the reduction on the back scan at E_{pc} = 0.52 V. The potentials of these oxidations are in close agreement with the oxidations of TPP (Table 1). Scanning to 1.5 V showed yet another small irreversible oxidation. This third multi-electron oxidation wave, near the background of the medium, is attributed to oxidation of the terminal ethynyl groups.[4] This oxidation resulted in the attachment of porphyrin to the glassy carbon electrode surface; attachment is only seen when the potential is scanned through the third oxidation. The collection of reduction data was overlooked and will be included future reports. The surface coverage after two scans to 1.5 V is typically $\Gamma = 3 \times 10^{-9}$ mol/cm^2.[16] Figures 6-8 show cyclic voltammograms of surface-bound TEPP while the electrode is immersed in a 0.1 M solution of [NBu_4][PF_6] in dichloromethane. The surface-bound TEPP has an

irreversible oxidation and a reversible oxidation (Table 1) (Fig. 6). A similar behavior is seen with the reductions; an irreversible reduction followed by a reversible reduction (Table 1) (Fig. 6). The potentials of the first reversible oxidations of solution and bound TEPP are within 0.06 V of each other, suggesting a similar redox process. Figure 7 shows only the reversible redox waves. These cyclic voltammograms were collected after first scanning positive (solid line) or negative (dashed line) depending if oxidations or reductions, respectively, were being studied. The irreversible processes are dependent on each other; in other words, the irreversible reduction can be regenerated by scanning through the irreversible oxidation and *vice versa*. Figure 8 shows the same scan (both scan in the negative direction and then the positive direction) performed successively. The first scan (solid line) had very little current for the reduction, while ~6 μA was measured for the oxidation. With the second scan (dashed line), a current of ~6 μA was observed, and the oxidation had nearly the same current as the previous scan. The ratio of the amount of charge passed in the irreversible processes compared to the reversible process varies between electrodes, and they are generally similar in magnitude to the reversible redox processes. The same behavior is seen when the potential is scanned in the positive direction first. This demonstrates that the irreversible waves can be regenerated.

Surface-bound TEPP went through a magnesium treatment outlined above to form surface-bound MgTEPP. The surface coverage of porphyrin decreased from $\Gamma = 3 \times 10^{-9}$ mol/cm^2 to $\Gamma = 1 \times 10^{-9}$ mol/cm^2 after treatment. Figures 9, 10, and 11 are the cyclic voltammetry of the MgTEPP electrode in a solution of $[NBu_4][PF_6]$ (0.1 M in dichloromethane). As with TEPP, an irreversible oxidation and reduction are seen (Table 1) (Fig. 10 and 11). These redox waves have the same dependency on each other; the oxidation wave regenerates the reduction wave and *vice versa*. Figures 10 and 11 show the results of consecutive scans; the large

irreversible waves are no longer present. Two reversible oxidations are observed (Table 1). The irreversible reduction (Table 1) was obscured by reduction seen in Figure 11, increasing the apparent current of the pre-wave. An ITO slide was modified with TEPP by the same method as the electrode. Figure 12 shows the UV-vis spectrum of the slide before (blue) and after (red) treatment with magnesium. The Soret bands for TEPP and MgTEPP are 425 nm and 431 nm, respectively, representing a 6-nm redshift. This is very similar to the 7-nm redshift seen with TPP and MgTPP.

Preparation of CoTEPP was attempted by the same method used for CoTPP. Four reversible reductions are present (Table 1) (Fig. 13, solid line). The second and fourth reductions are considerably smaller than the other reductions. There are no oxidations present (Fig. 13, dashed line). Scans out to 1.85 V do not yield oxidations of ethynyl groups. Therefore, no electrode attachment was achieved for CoTEPP.

Discussion:

The primary interest of this study was the preparation and characterization of surface-bound porphyrins. The prerequisite for surface attachment of a covalently-bounded porphyrins was the possession of terminal ethynyl groups. The syntheses, UV-vis spectra, and electrochemistry of TPP, MgTPP, CoTPP provided benchmarks for the ethynyl-terminated metal porphyrins, which are more difficult to obtain. Through oxidation of the ethynyl groups, the immobilization of porphyrins on a glassy carbon electrode was successfully achieved by methods outlined in the literature.[4] The electrochemistry (Fig. 7) and UV-vis spectra (Fig. 12) are in close agreement with reported data.

The first of covalently-bound magnesium porphyrins is reported here with the attachment of MgTEPP to glassy carbon. The magnesium treatment on the surface-bound TEPP yielded a redshift, 6 nm, in the UV-vis spectrum. A nearly identical redshift, 7 nm, is observed in dichloromethane with TPP and MgTPP.[12, 17] The attached MgTPP had similar redox properties as TEPP and was like the homogenous MgTPP, which had two reversible oxidations, ascribed to the ring, and an irreversible process, assigned to magnesium's reduction.[14] The separation between the first and second oxidations was 0.37 V and 0.36 V for MgTPP and surface-bound MgTEPP, respectively.

The reversible behavior of surface-bound TEPP was in close agreement with previous results (Fig. 7).[4] The irreversible waves were reported in supporting information of reference 4 and were attributed to electrode history (Fig. 8). These redox processes have also been described as "remnant negative charges,"[18] citing the existence of such waves with electrogenerated electroactive polymers.[19] M. Picot and coworkers described the surface-bound porphyrin as a polymer. A polymer is not an adequate description of the surface-bound porphyrin; porphyrin molecules are bonded to the electrode surface not to other porphyrin molecules. Remnant charge suggests that the attached porphyrin has a specific capacity, but no correlation was found between surface coverage

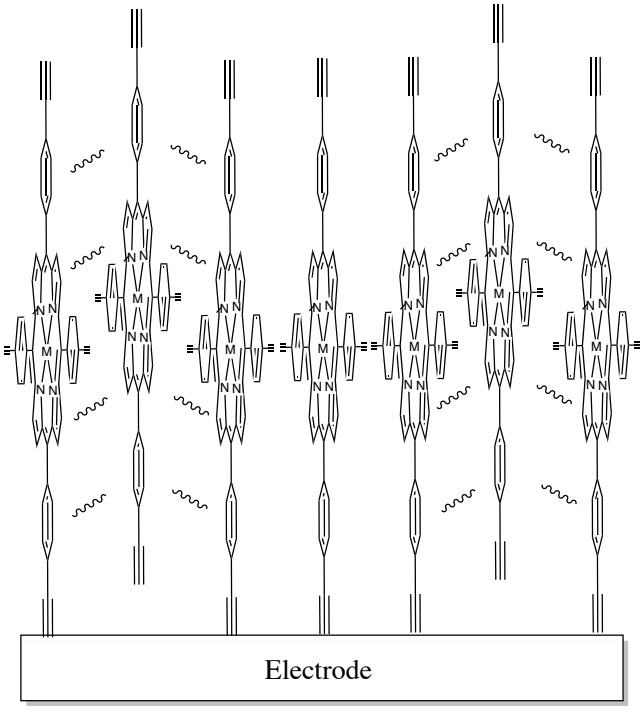

Scheme 5: 2D cut-away from the electrode surface, showing the hypothesized arrangement of the porphyrins. The π−stacking interactions shown with wavy bonds.

and the charge passed in the irreversible processes. Based on these data, we hypothesized that there are porphyrins immobilized near the electrode surface, which are not covalently attached. The sharp redox waves are reminiscent of adsorption/desorption waves.[20] Because the wave can be fully regenerated, the species do not defuse away, suggesting another mechanism immobilizing them. As the porphyrins are believed to be bound perpendicularly to the electrode surface,[21] we hypothesized that the porphyrins are prevented from defusing away by strong π-stacking interactions between the arene rings of the porphyrins. The number of non-covalently versus covalently attached porphyrins would be taken to be a stochastic process.

One of the goals of this project was the creation of surface-bound CoTEPP. It was originally hypothesized that a cobalt salt could be used to exchange MgTEPP's magnesium, because it was assumed that magnesium's large covalent radius[6] would make it loosely bonded. While there is precedent in the literature for magnesium metal exchange,[22] the kinetics are slow. When MgTPP was stirred with a 50-fold excess of $CoCl_2$, after 24 hours there was no discernable conversion to CoTPP (Fig. 1). Therefore, simple inorganic cobalt salts will not exchange with magnesium. CoTEPP was attempted to be synthesized for direct attachment to the electrode. Although the same procedure was used for the synthesis of CoTPP, the electrochemistry of the product was of doubtful veracity (Fig. 13). The cyclic voltammograms had little resemblance to those of CoTPP (Fig. 4). Therefore, we believed it is unlikely CoTEPP was synthesized, and it cannot be ruled out that oxidation of CoTEPP's ethynyl groups would yield attachment.

For future studies, electrodes modified with TEPP or MgTEPP will be tested in different media, systematically varying the solvent and supporting electrolyte. Other methods will be used

to synthesize CoTEPP, such as exchange with CdTEPP[23] or using the homogeneous synthesis methods.[11]

Reference:

1. Berger, D. J. *Science* **1999,** *286* (5437), 49.
2. Steele, B. C. H.; Heinzel, A. *Nature* **2001,** *414*, 345-352.
3. (a) Collman, J. P.; Denisevich, P.; Konai, Y.; Marrocco, M.; Koval, C.; Anson, F. C. *J. Am. Chem. Soc.* **1980,** *102*, 6027-6036; (b) Muthukumar, P.; John, S. A. *Electrochimica Acta* **2014,** *115*, 197-205; (c) Jiang, L.; Cui, L.; He, X. *J. Solid State Electrochem* **2015,** (19), 497-506.
4. Sheridan, M. V.; Lam, K.; Geiger, W. E. *Angew. Chem. Int. Ed.* **2013,** *52*, 12897-12900.
5. Reid, J.; Hambright, P. *Inorganica Chmica Acta* **1979,** *33*, L135-L136.
6. Cordero, B.; Gomez, V.; Platero-Prats, A. E.; Reves, M.; Echeverria, J.; Cremades, E.; Barragan, F.; Alvarez, S. *Dalton Trans* **2008**, 2832-2838.
7. Gritzner, G.; Kuta, J. *Pure and Applied Chemistry* **1984,** *56* (4), 461.
8. Gagne, R. R.; Koval, C. A.; Lisensky, G. C. *Inorganic Chemistry* **1980,** *19* (9), 2854-2855.
9. Drouet, S.; Merhi, A.; Yao, D.; Cifuentes, M. P.; Humphrey, M. G.; Wielgus, M.; Olesiak-Banska, J.; Matczyszyn, K.; Samoc, M.; Paul, F. e. e.; Paul-Roth, C. O. *Tetrahedron* **2012,** *68*, 10351-10359.
10. Lindsey, J. S.; Woodford, J. N. *Inorg. Chem.* **1995,** *34*, 1063-1069.
11. Mori, S.; Ishii, K.; Hirakawa, Y.; Nakamura, R.; Hashimoto, K. *Inorganic Chemistry* **2011,** *50* (6), 2037-2039.
12. Cissell, J. A.; Vaid, T. P.; Yap, G. P. A. *Organic Letters* **2006,** *8* (11), 2401-2404.
13. (a) Zhou, X.; Liu, D.; Wang, T.; Hu, X.; Guo, J.; Weerasinghe, K. C.; Wang, L.; Li, W. *Journal of Photochemistry and Photobiology A: Chemistry* **2014,** *274*, 57-63; (b) Paul-Roth, C.; Rault-Berthelot, J.; Simonneaux, G.; Poriel, C.; Abdalilah, M.; Letessier, J. *Journal of Electroanalytical Chemistry* **2006,** *597* (1), 19-27; (c) Potentials were converted from vs. SCH to vs. FcH through subtract by 0.46 V.
14. Takeda, J.; Sato, M. *Chemistry Letters* **1995,** *10*, 939-940.
15. Kadish, K. M.; Cornillon, J. L.; Yao, C. L.; Malinski, T.; Gritzner, G. *Journal of Electroanalytical Chemistry and Interfacial Electrochemistry* **1987,** *235*, 189-207.
16. Surface coverage (Γ) = C / nFA, where C is the charge (C), found through integration of the redox wave, n is the number of electrons, F is Faraday's constant (C/ mol), and A is the area of the electrode (cm^2).
17. Head, M. L.; Zarate, G.; Brückner, C. *European Journal of Organic Chemistry* **2016,** *2016* (5), 992-998.
18. Picot, M.; Nicolas, I.; Poriel, C.; Rault-Berthelot, J.; Barrière, F. *Electrochemistry Communications* **2012,** *20*, 167-170.
19. Rault-Berthelot, J.; Angely, L.; Delaunay, J.; Simonet, J. *New Journal of Chemistry* **1987,** *11* (6), 487 - 494.

20. (a) Soriaga, M. P.; Hubbard, A. T. *Journal of the American Chemical Society* **1982,** *104* (10), 2735-2742; (b) Coutanceau, C.; Croissant, M. J.; Napporn, T.; Lamy, C. *Electrochimica Acta* **2000,** *46* (4), 579-588.
21. Van Galen, D. A.; Majda, M. *Analytical Chemistry* **1988,** *60* (15), 1549-1553.
22. (a) Zvezdina, S. V.; Chizhova, N. V.; Mamardashvili, N. Z. *Russian Journal of General Chemistry* **2014,** *84* (4), 733-736; (b) Zvezdina, S. V.; Chizhova, N. V.; Mamardashvili, N. Z. *Russian Journal of General Chemistry* **2014,** *84* (10), 1989-1993.
23. (a) Berezin, B. D.; Rumyantseva, S. V.; Berezin, M. B. *Russian Journal of Coordination Chemistry* **2004,** *30* (4), 291-295; (b) Berezin, D. B.; Shukhto, O. V.; Reshetyan, M. S. *Russian Journal of General Chemistry* **2010,** *80*, 518-526.

Figures and Table:

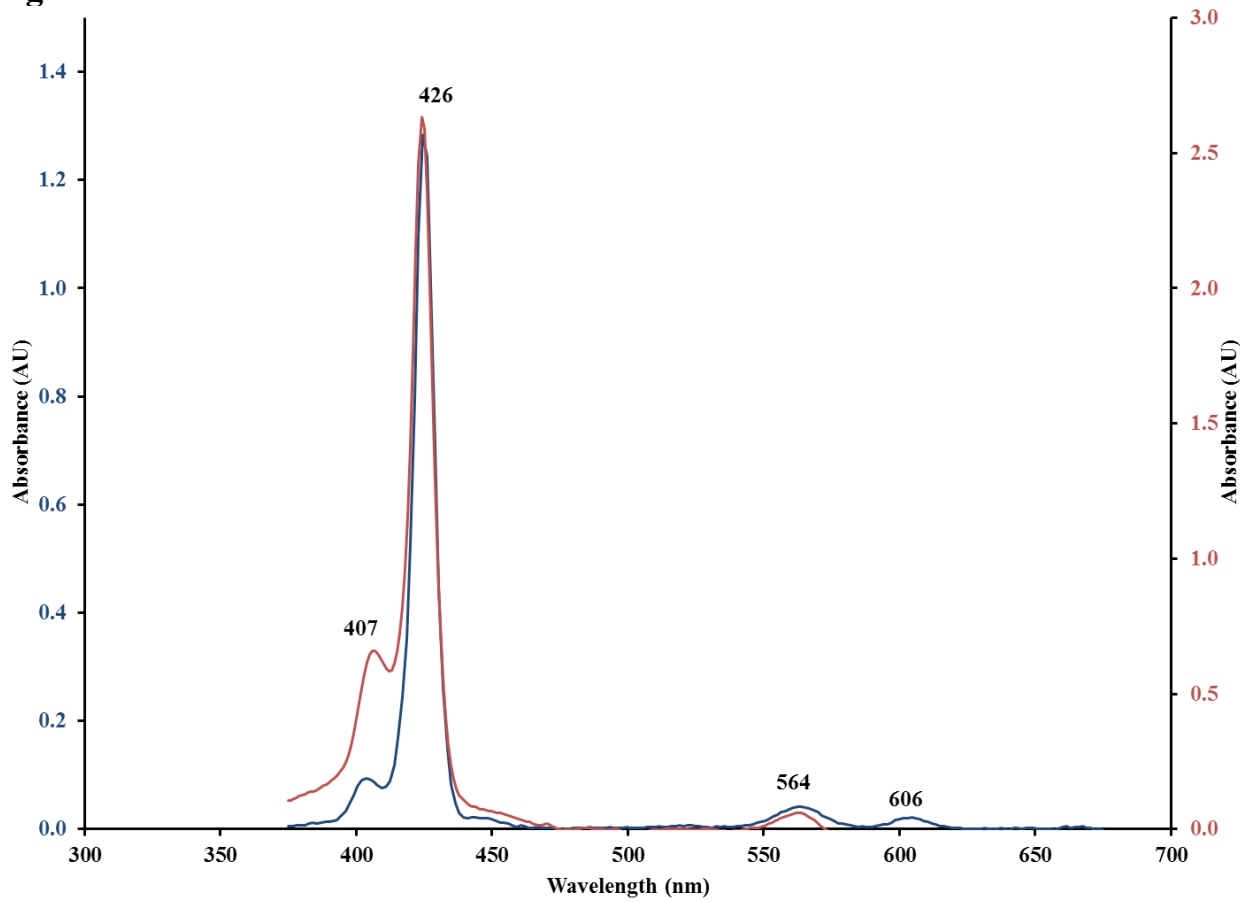

Figure 1: UV-vis spectra of a solution of MgTPP and a 50-fold excess of Co(II)Cl_2 initially (blue line) and after 24 hours (red line).

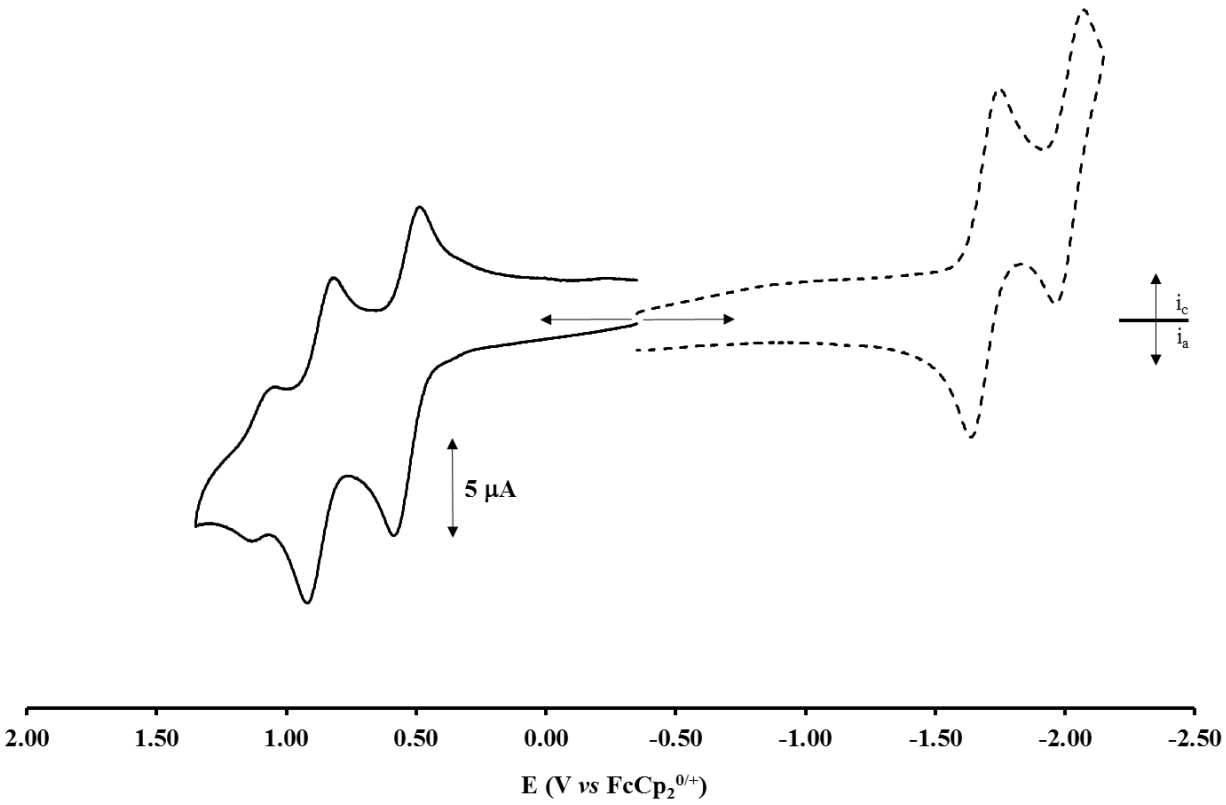

Figure 2: CV scans at 2 mm GC electrode, 0.2 V s^{-1}, in dichloromethane/0.1 M $[NBu_4][PF_6]$: 1 mM solution of TPP.

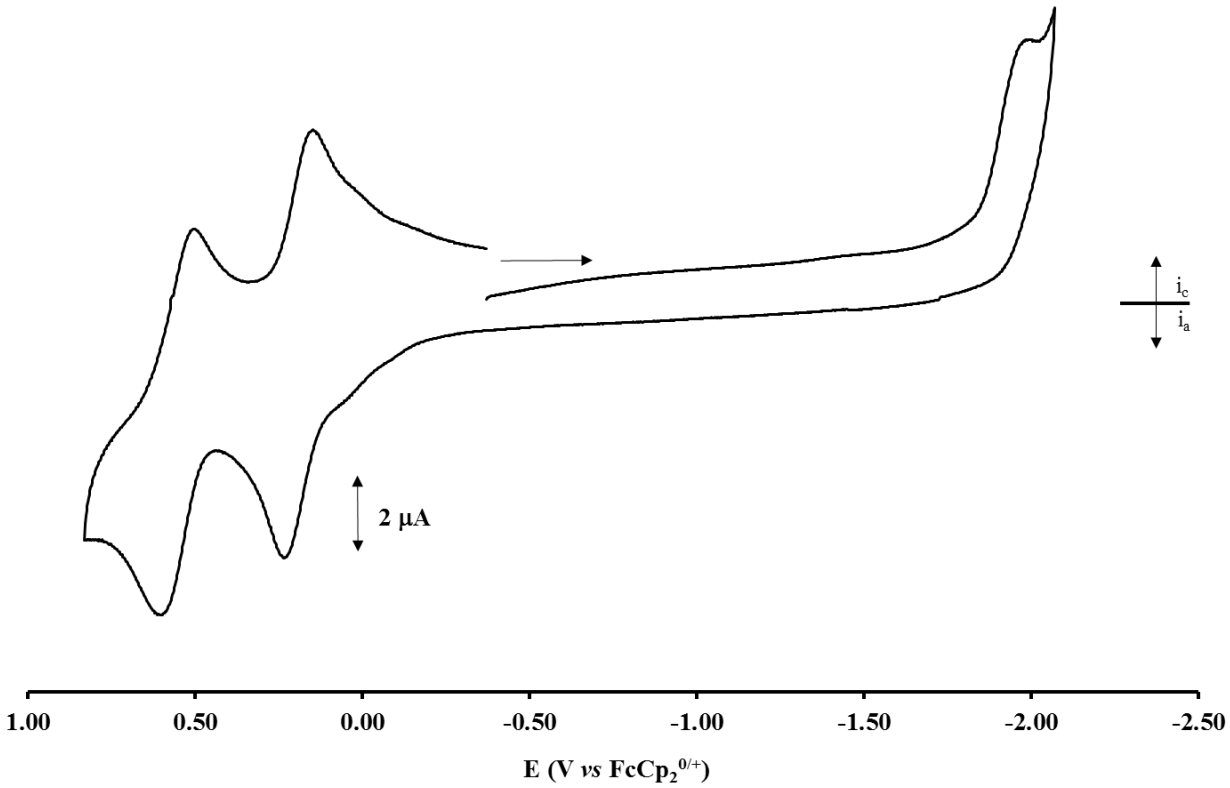

Figure 3: CV scans at 2 mm GC electrode, 0.2 V s^{-1}, in dichloromethane/0.1 M $[NBu_4][PF_6]$: 0.6 mM solution of MgTPP.

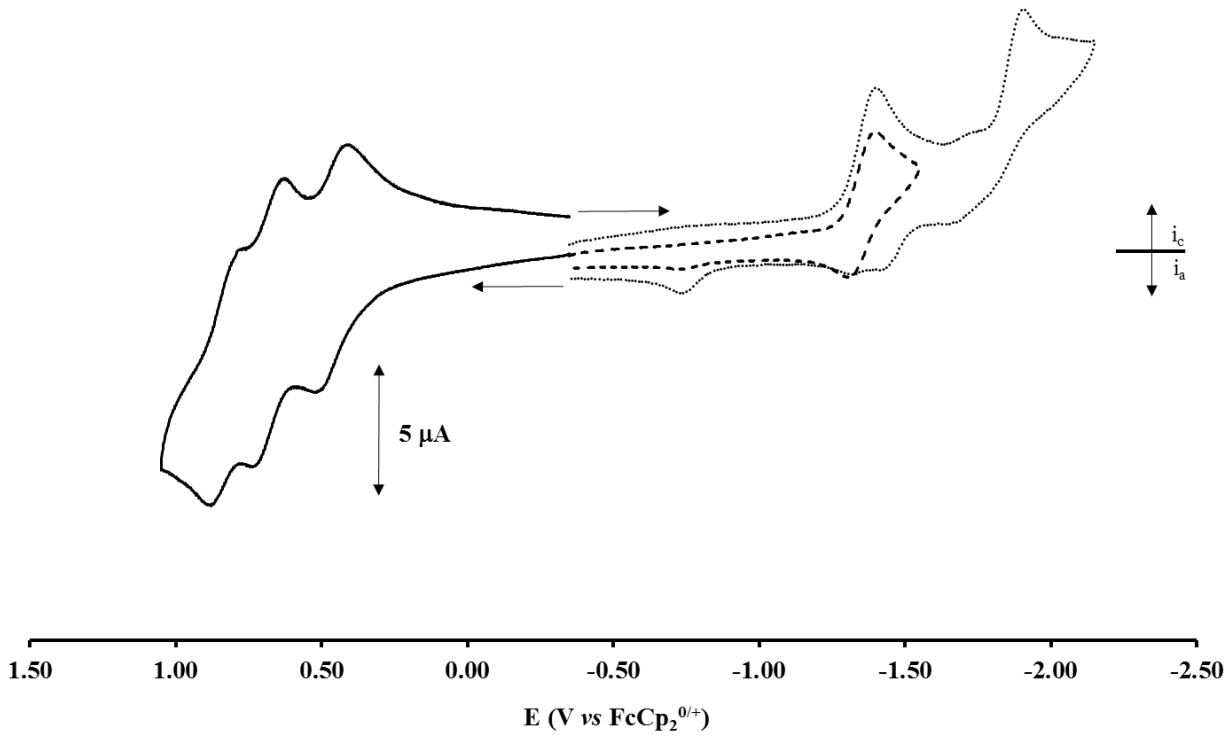

Figure 4: CV scans at 2 mm GC electrode, 0.2 V s^{-1}, in dichloromethane/0.1 M $[NBu_4][PF_6]$: 1 mM solution of CoTPP.

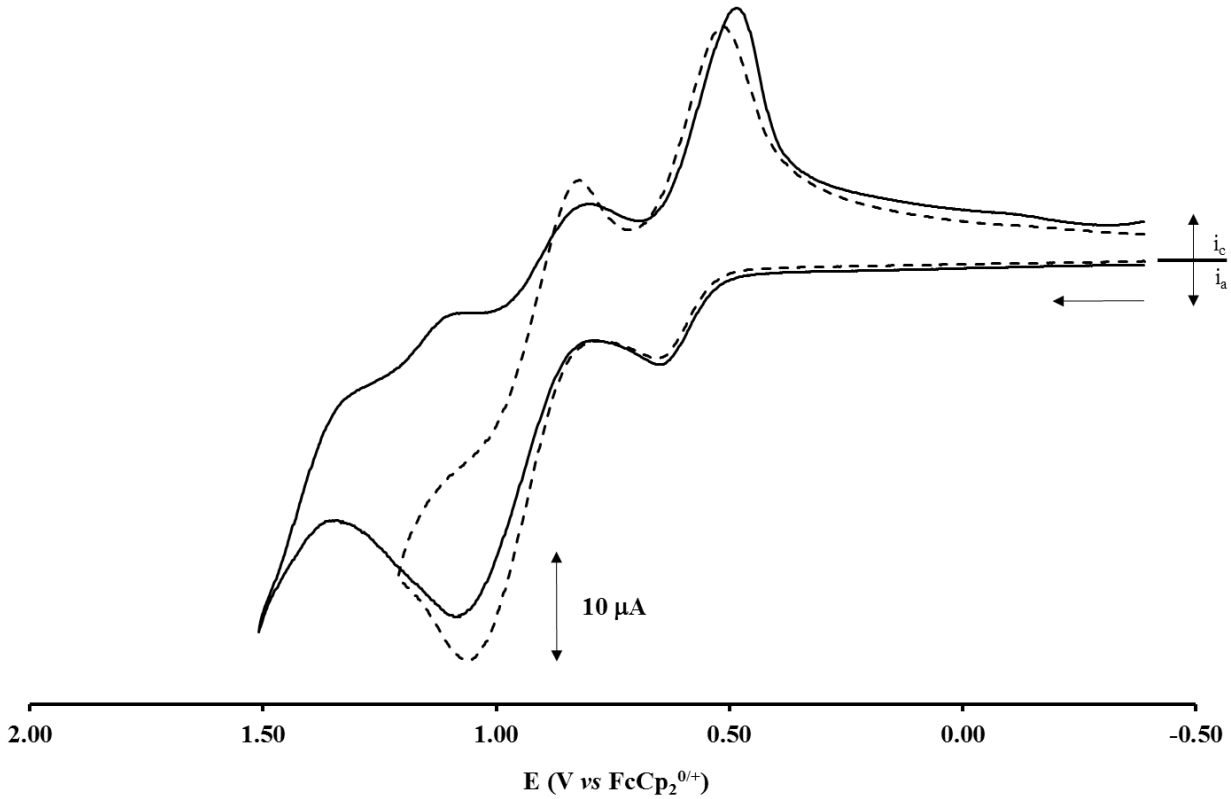

Figure 5: CV scans at 2 mm GC electrode, 0.2 V s^{-1}, in dichloromethane/0.1 M [NBu_4][PF_6]: 1 mM solution of TEPP.

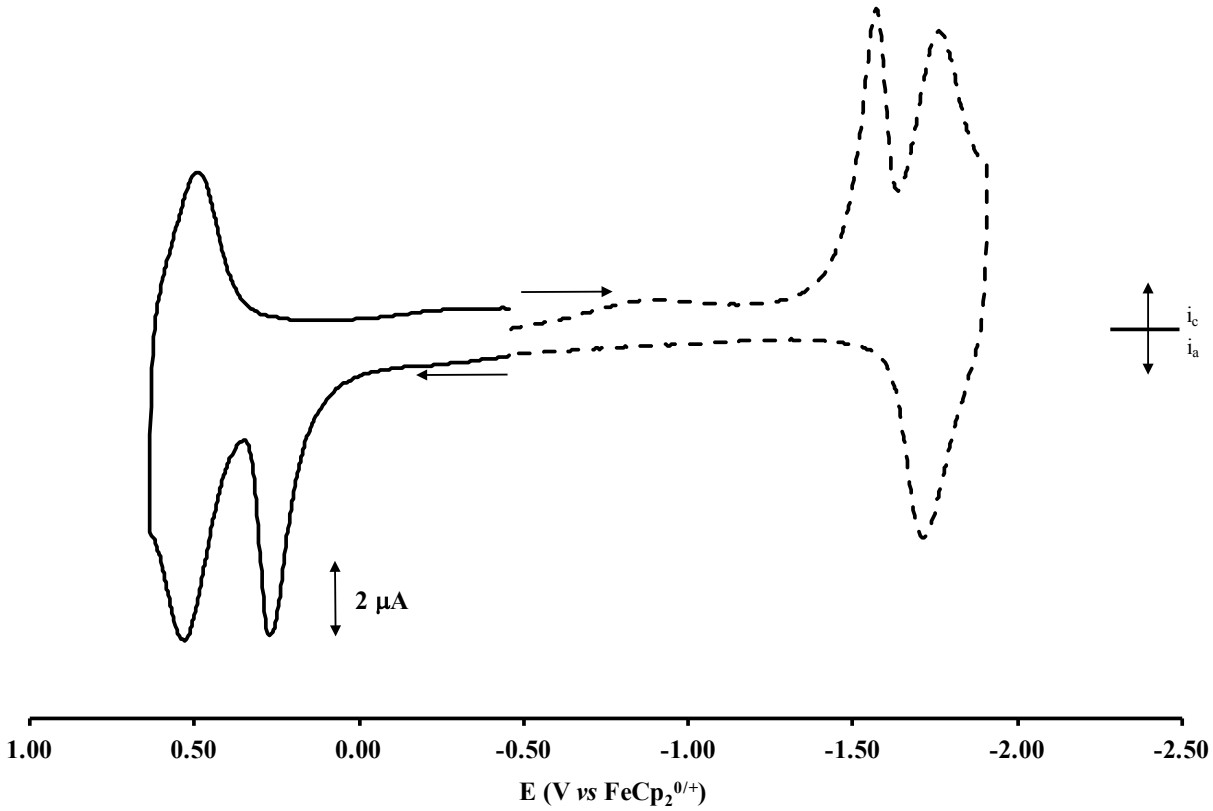

Figure 6: CV scans at 2 mm GC electrode modified with TEPP, 0.2 V s^{-1}, in dichloromethane/0.1 M $[NBu_4][PF_6]$.

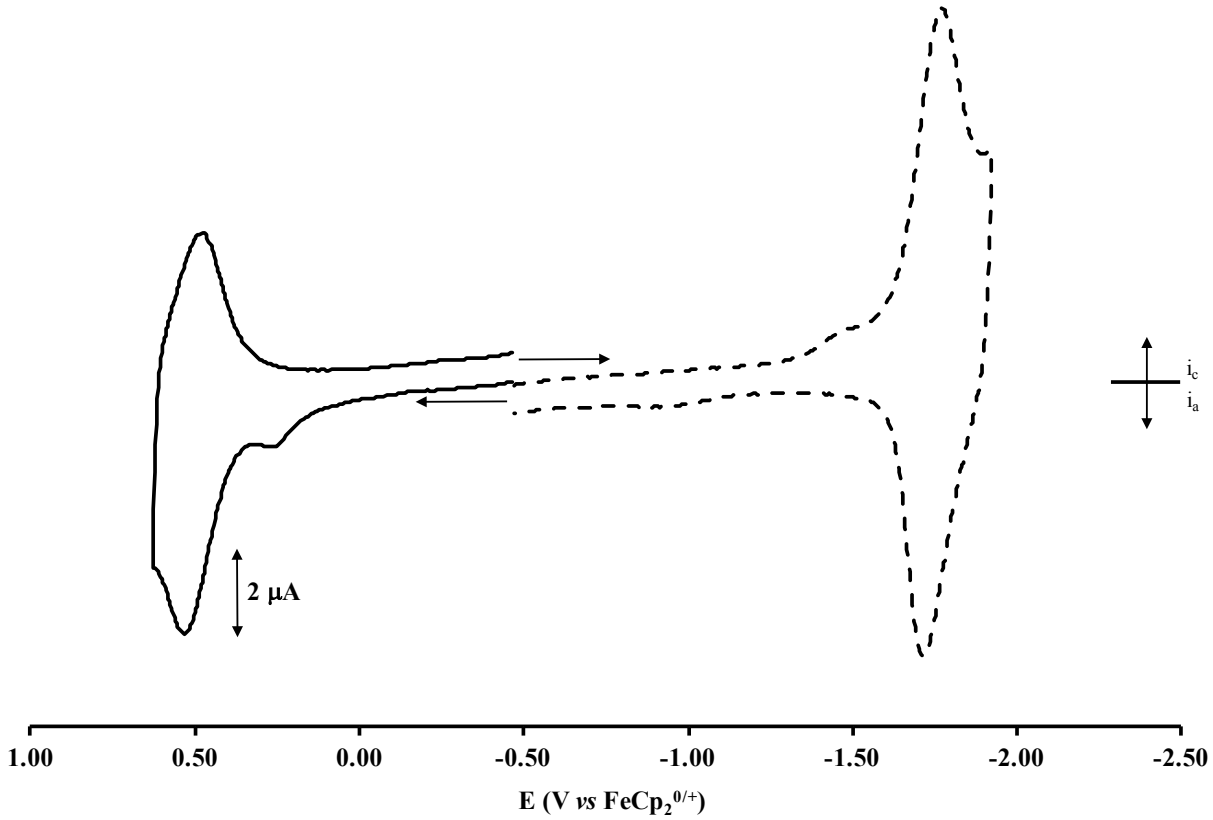

Figure 7: CV scans at 2 mm GC electrode modified with TEPP, 0.2 V s^{-1}, in dichloromethane/0.1 M $[NBu_4][PF_6]$.

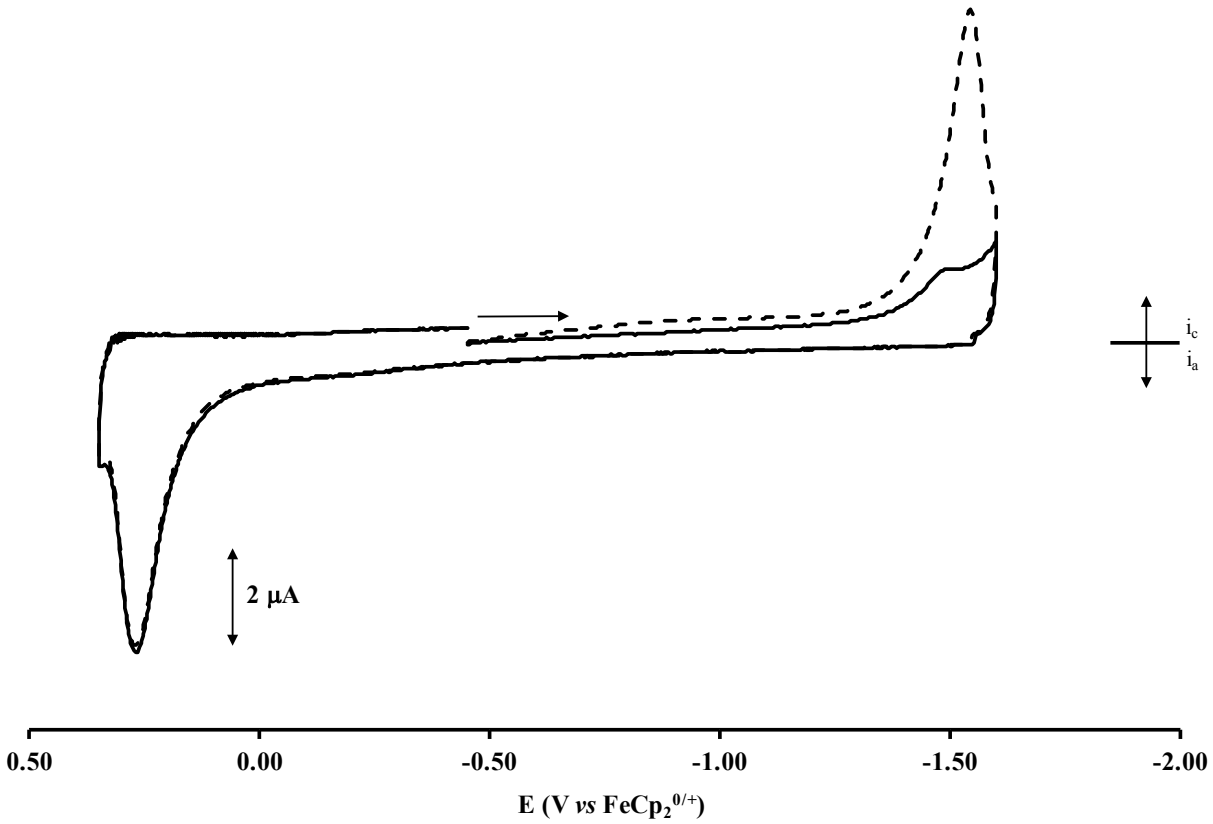

Figure 8: CV scans at 2 mm GC electrode modified with TEPP, 0.2 V s^{-1}, in dichloromethane/0.1 M [NBu_4][PF_6]: first scan (solid line), second scan (dashed line).

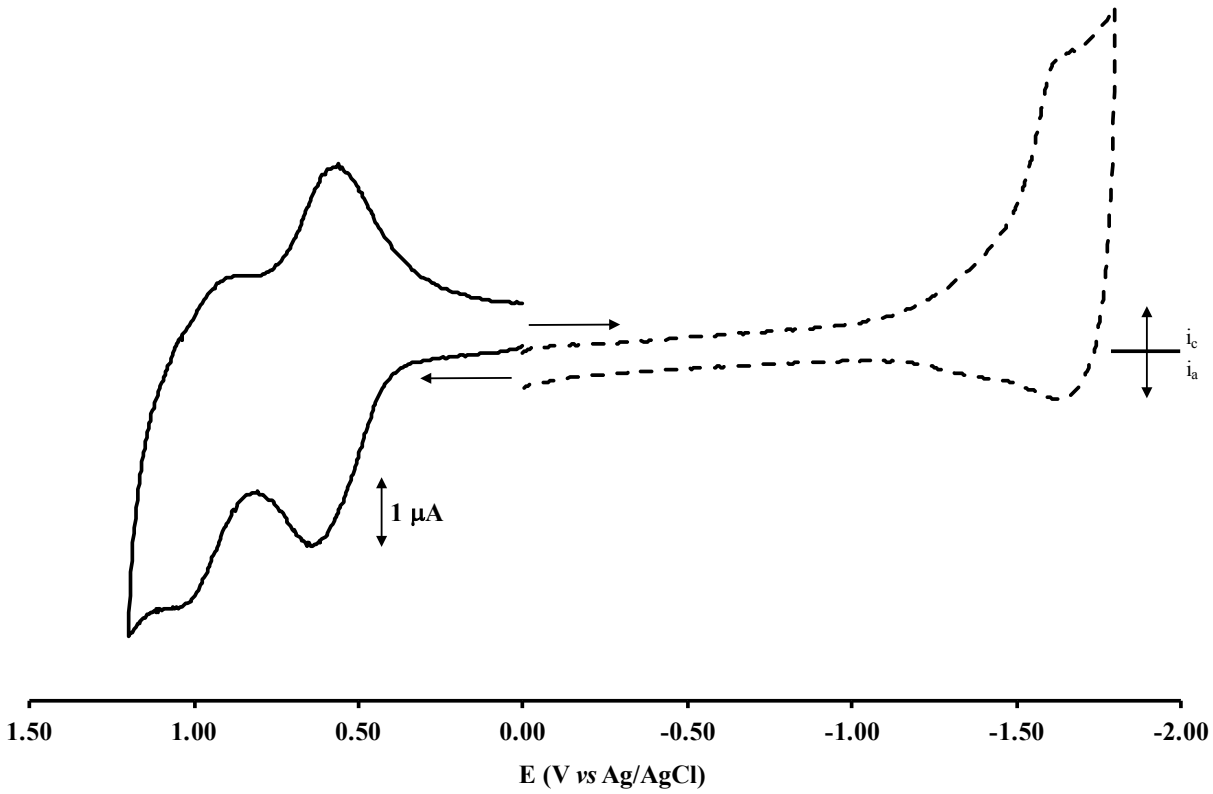

Figure 9: CV scans at 2 mm GC electrode modified with MgTEPP, 0.2 V s^{-1}, in dichloromethane/0.1 M $[NBu_4][PF_6]$.

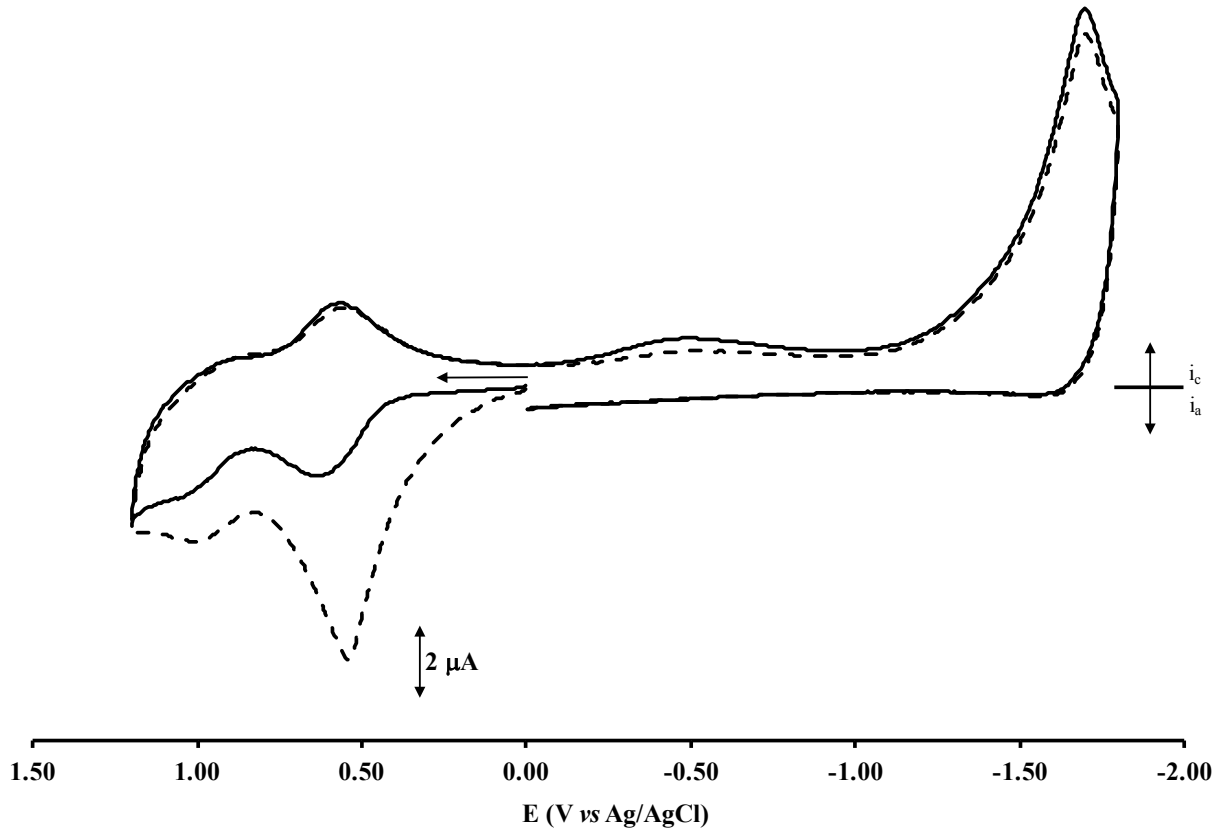

Figure 10: CV scans at 2 mm GC electrode modified with MgTEPP, 0.2 V s^{-1}, in dichloromethane/0.1 M [NBu_4][PF_6]: first scan (solid line), second scan (dashed line).

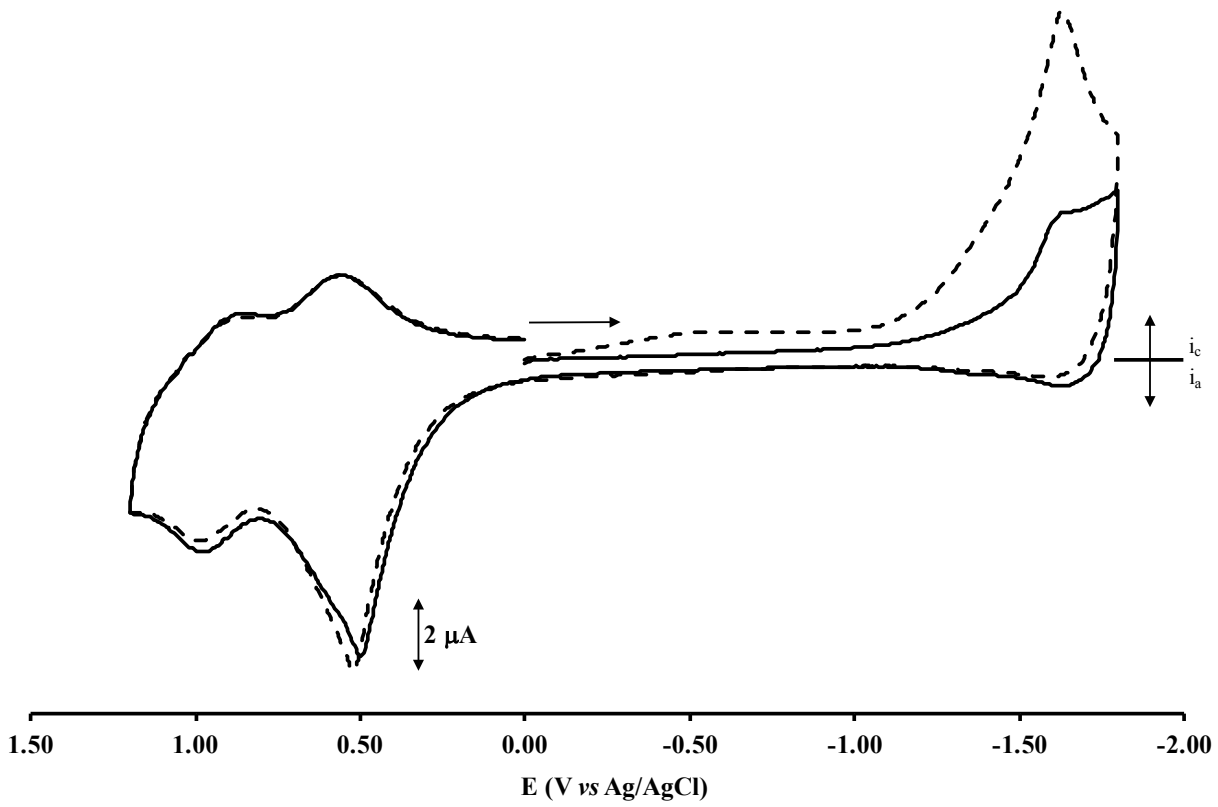

Figure 11: CV scans at 2 mm GC electrode modified with MgTEPP, 0.2 V s^{-1}, in dichloromethane/0.1 M [NBu_4][PF_6]: first scan (solid line), second scan (dashed line).

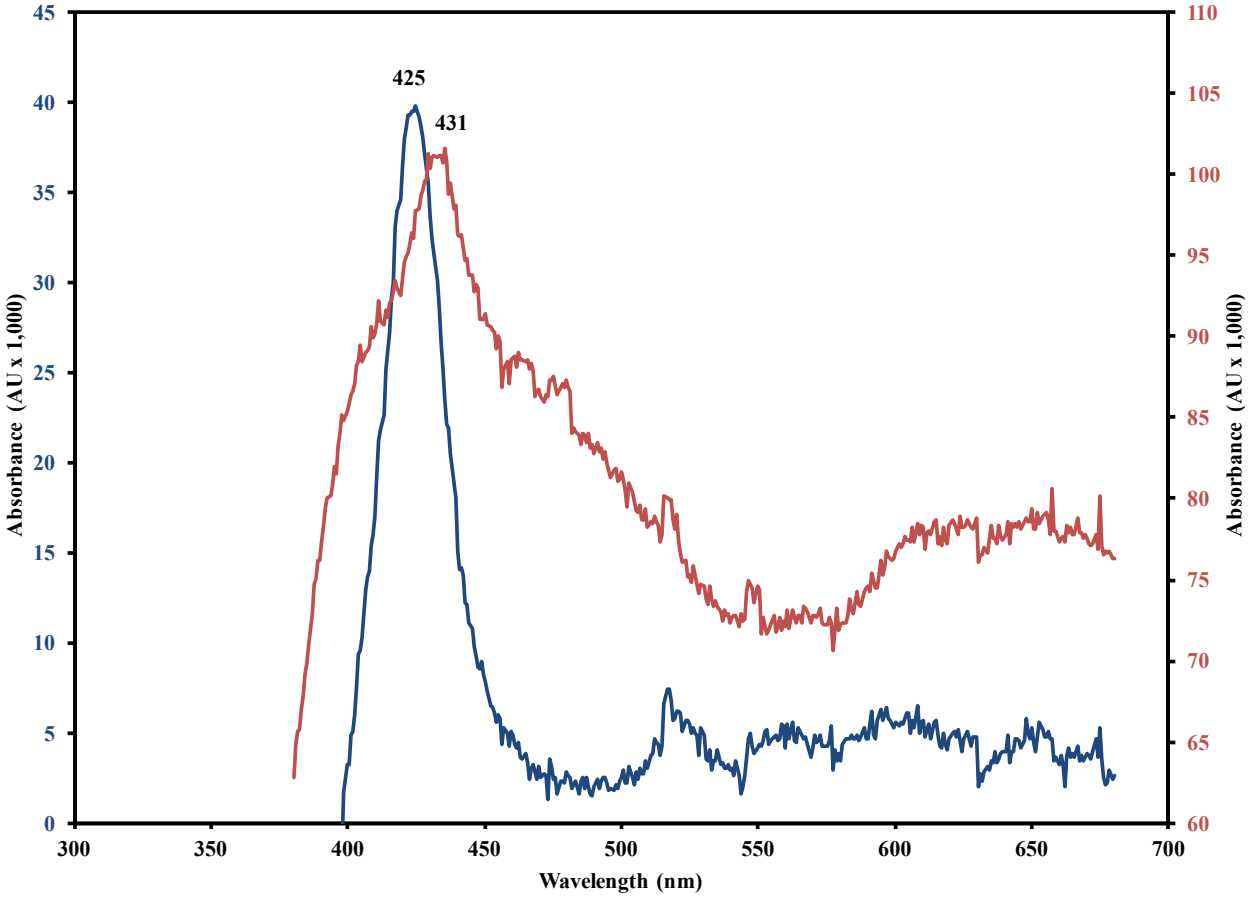

Figure 12: UV-vis spectra of an ITO slide modified with TEPP (blue line) and after Mg treatment (red line).

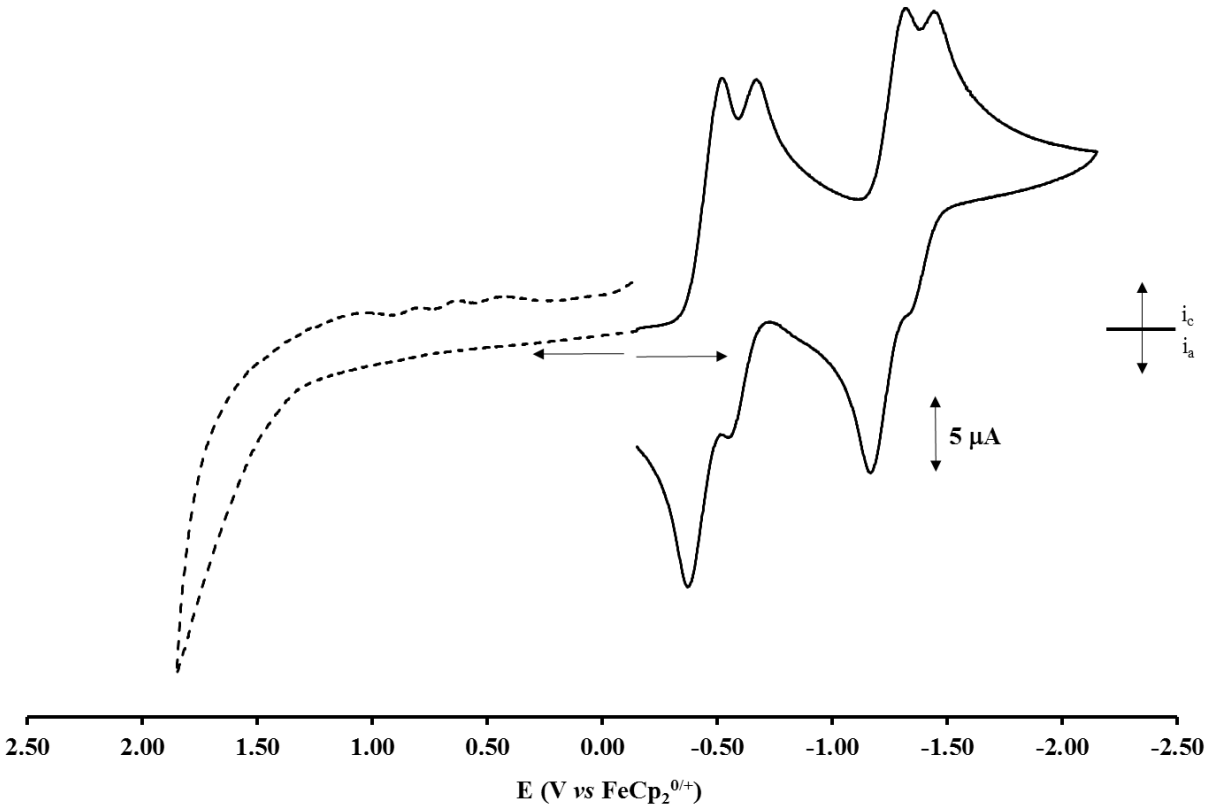

Figure 13: CV scans at 2 mm GC electrode, 0.2 V s^{-1}, in dichloromethane/0.1 M $[NBu_4][PF_6]$: 1 mM solution of CoTEPP.

Table 1: The potentials versus ferrocene, unless otherwise noted, of the various redox processes for each compound. The measurements were made in dichloromethane/ 0.1 M $[NBu_4][PF_6]$. **a:** Irreversible process, 0.2 V s^{-1}. **b:** Surface-bound porphyrin. **c:** Referenced vs. Ag/AgCl.

	TPP	**MgTPP**	**CoTPP**	**TEPP**	**TEPP[b]**	**MgTEPP[b]**	**CoTEPP**
3rd Oxidation	-	-	0.84 V	>1.50 V	-	0.97 V[c]	-
2nd Oxidation	0.87 V	0.56 V	0.69 V	0.94 V	0.52 V	0.61 V[c]	-
1st Oxidation	0.54 V	0.19 V	0.46 V	0.58 V	0.28 V[a]	0.50 V[a,c]	-
1st Reduction	-1.70 V	-1.98 V[a]	-1.36 V	-	-1.57 V[a]	-1.62 V[a,c]	-0.45 V
2nd Reduction	-2.02 V	-	-1.90 V[a]	-	-1.74 V	-1.65 V[a,c]	-1.25 V